Loss-of-Function Variants in *PPP1R12A*: From Isolated Sex Reversal to Holoprosencephaly Spectrum and Urogenital Malformations

Joel J. Hughes,[1,22] Ebba Alkhunaizi,[2,3,22] Paul Kruszka,[1,*] Louise C. Pyle,[4] Dorothy K. Grange,[5] Seth I. Berger,[1,6,7] Katelyn K. Payne,[8] Diane Masser-Frye,[9] Tommy Hu,[1] Michelle R. Christie,[10] Nancy J. Clegg,[10] Joshua L. Everson,[11,12] Ariel F. Martinez,[1] Laurence E. Walsh,[8] Emma Bedoukian,[4] Marilyn C. Jones,[9] Catharine Jean Harris,[13] Korbinian M. Riedhammer,[14,15] Daniela Choukair,[16] Patricia Y. Fechner,[17] Meilan M. Rutter,[18] Sophia B. Hufnagel,[19,21] Maian Roifman,[2,3] Gad B. Kletter,[20] Emmanuele Delot,[6,7] Eric Vilain,[6,7] Robert J. Lipinski,[11,12] Chad M. Vezina,[11,12] Maximilian Muenke,[1] and David Chitayat[2,3]

In two independent ongoing next-generation sequencing projects for individuals with holoprosencephaly and individuals with disorders of sex development, and through international research collaboration, we identified twelve individuals with *de novo* loss-of-function (LoF) variants in protein phosphatase 1, regulatory subunit 12a (*PPP1R12A*), an important developmental gene involved in cell migration, adhesion, and morphogenesis. This gene has not been previously reported in association with human disease, and it has intolerance to LoF as illustrated by a very low observed-to-expected ratio of LoF variants in gnomAD. Of the twelve individuals, midline brain malformations were found in five, urogenital anomalies in nine, and a combination of both phenotypes in two. Other congenital anomalies identified included omphalocele, jejunal, and ileal atresia with aberrant mesenteric blood supply, and syndactyly. Six individuals had stop gain variants, five had a deletion or duplication resulting in a frameshift, and one had a canonical splice acceptor site loss. Murine and human *in situ* hybridization and immunostaining revealed *PPP1R12A* expression in the prosencephalic neural folds and protein localization in the lower urinary tract at critical periods for forebrain division and urogenital development. Based on these clinical and molecular findings, we propose the association of *PPP1R12A* pathogenic variants with a congenital malformations syndrome affecting the embryogenesis of the brain and genitourinary systems and including disorders of sex development.

Protein phosphatase 1, regulatory subunit 12a (*PPP1R12A* [MIM: 602021]) encodes a component of myosin phosphatase (MP), a key enzyme instrumental in the regulation of cell morphology and motility.[1,2] PPP1R12A interacts with the protein phosphatase type 1 catalytic unit (PP1c) and M20/21 to form MP, which is a trimeric holoenzyme. MP regulates the function of non-muscle myosin II by regulating the phosphorylation state of myosin regulatory light chain.[3–5] MP activates when PP1c is unphosphorylated and bound. Phosphorylation of specific consensus sites on PPP1R12A by protein kinases leads to inhibition of its activity. Pathogenic variants in *PPP1R12A* prevent PPP1R12A from binding to PP1c and result in a non-functional MP.[6] Since the initial discovery of MP,[5,7] research to define its characterization and function has been productive, but the application of these findings to human diseases has been limited. Previously published animal models illustrate an instrumental role of PPP1R12A during embryogenesis through the regulation of cell movement and adhesion. The mutated *Drosophila* homologue of *PPP1R12A (DMYPT)* demonstrates that this protein is required for cell movement during dorsal closure and morphogenesis of the eye.[8,9] In *C. elegans*, PPP1R12A homologue MEL-11 facilitates embryonic elongation through changes in cell shape by contraction of the epidermal cell layer that encloses the embryo.[10] In mice, targeted

[1]Medical Genetics Branch, National Human Genome Research Institute, National Institutes of Health, Bethesda, MD 20892, USA; [2]The Prenatal Diagnosis and Medical Genetics Program, Department of Obstetrics and Gynecology, Mount Sinai Hospital, University of Toronto, Toronto, Ontario, M5G 1X5, Canada; [3]Division of Clinical and Metabolic Genetics, Department of Pediatrics, The Hospital for Sick Children, University of Toronto, Toronto, Ontario, M5G 1X8, Canada; [4]Division of Human Genetics, Children's Hospital of Philadelphia, Philadelphia, PA 19104, USA; [5]Department of Pediatrics, Division of Genetics and Genomic Medicine, Washington University School of Medicine, St. Louis, MO, 63110, USA; [6]Center for Genetic Medicine Research, Children's National Hospital, Washington, DC 20010, USA; [7]Department of Genomics and Precision Medicine, George Washington University, Washington, DC 20037, USA; [8]Division of Child Neurology, Riley Hospital for Children, Indianapolis, Indiana, 46202, USA; [9]Department of Pediatrics, Division of Genetics, University of California San Diego—Rady Children's Hospital, San Diego, CA 92123, USA; [10]Texas Scottish Rite Hospital for Children, Dallas, TX 75219, USA; [11]Department of Comparative Biosciences, School of Veterinary Medicine, University of Wisconsin—Madison, Madison, WI 53706, USA; [12]Molecular and Environmental Toxicology Center, University of Wisconsin—Madison, Madison, WI 53706, USA; [13]Department of Pediatric Genetics, University of Missouri Medical Center, Columbia, MO 65212, USA; [14]Institute of Human Genetics, Klinikum rechts der Isar, Technical University of Munich, Munich, 4JQ2+9Q, Germany; [15]Department of Nephrology, Klinikum rechts der Isar, Technical University of Munich, Munich, 4JQ2+9Q, Germany; [16]Division of Paediatric Endocrinology and Diabetology, University Children's Hospital, 69120 Heidelberg, Germany; [17]Division of Pediatric Endocrinology, Seattle Children's Hospital, University of Washington, Seattle, WA 98105, USA; [18]Division of Endocrinology, Cincinnati Children's Hospital Medical Center, University of Cincinnati College of Medicine, Cincinnati, OH 45229, USA; [19]Rare Disease Institute, Children's National Hospital, Washington, DC 20010, USA; [20]Pediatric Endocrinology, Mary Bridge Children's Hospital, Tacoma, WA 98404, USA
[21]Present Address: Food and Drug Administration, Silver Spring, MD 20993, USA
[22]These authors contributed equally to this work
*Correspondence: paul.kruszka@nih.gov
https://doi.org/10.1016/j.ajhg.2019.12.004.

disruption of *Ppp1r12a* results in embryonic lethality before 7 days post conception.[11] Lastly, zebrafish *ppp1r12a* morpholino knockdown results in gastrulation defects including complete and partial cyclopia, partial cyclopia, and microphthalmia reminiscent of the severe phenotypic changes observed in humans with holoprosencephaly (HPE).[12] We report the association of loss-of-function (LoF) variants in *PPP1R12A* with multiple congenital anomalies, including HPE spectrum and urogenital malformations.

Twelve individuals with *de novo* LoF variants in *PPP1R12A* were identified by multiple clinical genetic centers in the United States, Canada, and Europe and evaluated by clinical exam, brain imaging (when clinically indicated), and/or autopsy. Clinical and research laboratories identified variants by exome sequencing (see Supplemental Materials and Methods in Supplemental Information). This study was approved by the National Human Genome Research Institute Institutional Review Board (IRB), Children's National Health System IRB, and local IRBs. Informed consent for publication was obtained from all individuals or legal guardians. The clinical manifestations in twelve individuals with *de novo* heterozygous LoF variants in *PPP1R12A* are summarized in Table 1 and described as follows (see Supplemental Note—Case Reports in Supplemental Information). The first two individuals originated from an HPE cohort of 277 individuals (135 trios and 142 singletons).[13] Per protocol, Sanger sequencing of the four most common genes associated with HPE, *SHH* (MIM: 600725), *ZIC2* (MIM: 603073), *SIX3* (MIM: 603714), and *TGIF1* (MIM: 602630), failed to identify any detectable pathogenic variants (see Supplemental Materials and Methods in Supplemental Information). Individual 1 had syntelencephaly or middle interhemispheric variant (MIHV) of HPE, polymicrogyria, and Chiari I malformation identified on brain MRI, as well as other medical diagnoses including intellectual disability, attention deficit hyperactivity disorder (ADHD), and seizures. Individual 2 had semilobar HPE and agenesis of the corpus callosum identified on MRI, and other medical diagnoses included myoclonus, intellectual disability, and syndactyly of the toes. Data from individuals 3 through 10 were obtained through GeneMatcher.[14] In addition to agenesis of the corpus callosum and colpocephaly in the third individual and fetal acrania with exencephaly and omphalocele in the fourth individual, inclusion of urogenital anomalies and a spectrum of 46,XY disorders of sex development (DSD) was seen in individuals 5 through 10. Individuals 11 and 12 were identified through a targeted variant search in a cohort of 94 families (300 individuals) with DSD. While chromosomal sex on either CMA or karyotype was normal male on these last two individuals, their urogenital phenotypes ranged from streak gonads, rudimentary Fallopian tubes, and a urogenital sinus to ovaries which underwent gonadal degeneration, a uterus, posterior labial fusion, a clitoris, and increased labial rugation with pigmentation. Seven of 12 individuals in this study had developmental delay (Table 1: individuals 1,2,6,7,10,11, and 12); however, two of these individuals had unremarkable brain MRIs (individuals 10 and 11), and this implies that other mechanisms besides structural brain anomalies may be responsible for developmental delay. The variants in *PPP1R12A* from each of these individuals are noted in Table 1, and their positions and domains are annotated along the protein in Figure 1.

Brain *in situ* hybridization in mouse revealed *Ppp1r12a* expression in the prosencephalic neural folds of the mouse at gestational day (GD) 8.25. Staining of sections through the neural folds illustrated *Ppp1r12a* expression restricted to the mesenchymal compartment (Figure 2). Next, examination of *Gli2* expression occurred on the same tissues as a positive control. *Gli2* encodes the dominant Shh pathway transcriptional activator, and LoF variants in this gene cause HPE in both humans and mice.[16–19] *Gli2* was expressed in the head mesenchyme adjacent to the prosencephalic neuroectoderm. These results demonstrate that *Ppp1r12a* is expressed in the prosencephalic neural folds during the critical period for HPE in a pattern consistent with known HPE-associated genes. Mouse urogenital immunostaining of PPP1R12A showed protein localization in the lower urinary tract, specifically in epithelium of the bladder, urethra, and genital tubercle epithelium at GDs 13 and 13.75 (Figures 3A and 3C). Immunohistochemical (IHC) staining was also conducted for PPP1R12B (MIM: 603768), which is an isoform of PPP1R12A. PPP1R12B localization was not seen in the urogenital tract at GD 13 (Figure 3B) or GD 13.75 (Figure 3D). In human embryos at week 10, IHC staining revealed PPP1R12A localization in the genital tubercle epithelium (ectoderm derived), the bladder and urethra (endoderm derived), urogenital sinus (UGS) mesenchymal cells, and bladder detrusor muscle (Figure 3E). PPP1R12B protein localization was restricted to the bladder detrusor smooth muscle (Figure 3F). These results show unique localization of PPP1R12A in the lower urinary tract during urethral development in advance of urethral plate closure.

In summary, we present 12 individuals with LoF variants in *PPP1R12A* and multiple congenital anomalies. The two most common affected organ systems are the brain and the genitourinary tract. Five of the 12 individuals (~40%) had midline brain anomalies found via MRI, and two individuals had HPE (individuals 1 and 2); the most severe brain finding was anencephaly (individual 4). Nine affected individuals (75%) had genitourinary malformations including three 46,XY individuals with female external genitalia. Only two individuals had both brain and genitourinary anomalies (individuals 6 and 7).

Among these individuals, there is a broad spectrum of manifestations, and a clear genotype-phenotype correlation was not seen associating with specific variants in *PPP1R12A*. The variants occurred across multiple exons (1, 5, 6, 9, 10, 11, 15, 18, and 21) as well as in intron 5. Two variants occurred in the ankyrin repeat domains, and two occurred in the rho-associated coiled-coil kinase

Table 1. Summary of Neurologic and Urogenital Phenotypes

-	1	2	3	4	5	6	7	8	9	10	11	12
Age	15 years	15 years	5.5 years	12 weeks gestation	3 years	6 years	7 years	45 years	2 years	2 years	12 years	3 years
Brain malformation	MIHV HPE	semilobar HPE	agenesis of the corpus callosum	acrania, anencephaly	head CT unremarkable	dysgenesis of the corpus callosum, absent septum pellucidum, Chiari malformation, cortical dysplasia/ polymicrogyria, and grey matter heterotopia	leukomalacia	not evaluated	not evaluated	brain MRI unremarkable	brain MRI unremarkable	not evaluated
Genitourinary malformation	not evaluated	not evaluated	renal asymmetry	not described on autopsy	micropenis, chordee, scrotal hypospadias, bilateral cryptorchidism, and uterus	glandular hypospadias and chordee	hypospadias, cryptorchidism, uterus and ovaries	uterine didelphys and streak gonads	clitoral hypertrophy, UGS, posterior fusion of the labia majora	grade 2 hypospadias, cryptorchidism, removal of right inguinal hernia identified as a fallopian tube, and uterus	streak gonads with rudimentary fallopian tubes, and UGS	clitoris, posterior labial fusion, labial rugation and pigmentation, uterus, fallopian tubes and ovaries
Head and facial features	macrocephaly, hypertelorism	microcephaly, epicanthal folds, long philtrum	not described	hypertelorism, flattened facial profile, absent nasal bone	not described	short upslanting palpebral fissures, low-set ears, and micrognathia	long face, large protruding ears, ptosis, small pointed nose	not described	not described	not described	not described	deformed pinnae, epicanthus inversus
Other	Developmental delay	developmental delay, syndactyly	ADHD, kyphoscoliosis, stiff joints, decreased subcutaneous fat	omphalocele	absent	developmental delay, strabismus, astigmatism, hyperopia, and alternating esotropia	developmental delay, bilateral rod and cone dysfunction, decreased vision, and latent nystagmus	absent	absent	developmental delay	developmental delay	developmental delay, strabismus, right esotropia
Genotypic sex	46,XX	46,XX	46,XY	46,XX	46,XY	46,XY	46,XY	46,XY	46,XY	46,XY	46,XY	46,XY
Phenotypic sex	female	female	male	female	male	male	male	female	female	male	female	female
Inheritance	*de novo*	unknown	*de novo*	*de novo*	*de novo*	*de novo*	unknown	unknown	*de novo*	*de novo*	*de novo*	*de novo*
Variant	c.2033_ 2034delCT (p.Ser678*)	c.1415C>G (p.Ser472*)	c.793-1G>A	c.223_224delAC (p.Thr75Cysfs*8)	c.2739_2740delCT (p.Leu914Argfs*14)	c.1510C>T (p.Arg504*)	c.2573G>A (p.Trp858*)	c.2073dupA (p.Ser692Ilefs*2)	c.2698C>T (p.Arg900*)	c.960dupA (p.Glu321Argfs*6)	c.1189delA (p.Thr397Hisfs*42)	c.681dupT (p.Lys228*)

Individuals 1–4 share the neurological phenotype, individuals 3 and 5–12 share diverse urogenital malformations, and individuals 3, 6, and 7 share an overlap of both. Notable discordance in genotypic and phenotypic sex is seen between the 46,XX and 46,XY individuals, but the significance requires further investigation. Transcript NM_002480.3 was used for all described variants in *PPP1R12A*. Abbreviations: MIHV—middle interhemispheric variant, HPE—holoprosencephaly, ADHD—attention deficit hyperactivity disorder, and UGS—urogenital sinus.

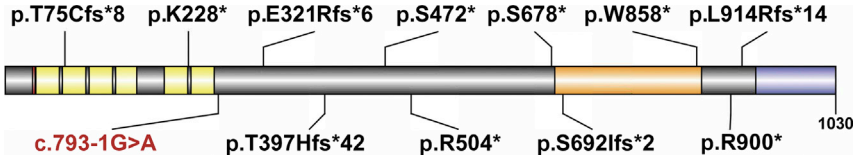

Figure 1. PPP1R12A with Variant Annotations and Highlighted Regions
Per UniProt, domains include a Lysine-Valine-Lysine-Phenylalanine (KVKF) motif (red), multiple ankyrin repeats (yellow), rho-associated coiled-coil-containing protein kinase 1 (ROCK1) and rho-associated coiled-coil-containing protein kinase 2 (ROCK2) interaction site (orange), and a leucine zipper domain which binds a cGMP-dependent protein kinase 1. Stop gain and frameshift variants are notated in black with the splice-site variant in red at the approximate site predicted to result in a premature termination codon and nonsense-mediated decay. Diagram was created using Domain Graph version 2.0.[15]

binding domains without an observable pattern between the phenotypes. Premature termination codon (PTC) with subsequent nonsense-mediated decay (NMD) was predicted for the stop gain and frameshift variants because these followed the previously described criteria for this mechanism.[20,21] *In silico* modeling of the splice-site variant predicted canonical splice acceptor site destruction in intron 5 with secondary PTC and NMD. Tissue-specific mRNA expression patterns were not available for individuals in this study, and review of a prior expression study on human fetal samples did not specifically include brain or urogenital tissue.[22] As such, the value of comparing expression of *PPP1R12A* in adult tissues to expression during fetal development is limited because the impact leading to the observed phenotypes may be most influenced by these initial alterations. Review of DECIPHER revealed copy-number variants (CNV) of various sizes involving *PPP1R12A*. Neurologic and urogenital phenotypes were noted, but direct comparison of these CNVs remains limited due to the limited ability to quantify the haploinsufficiency from each of the other deleted genes. 12q21 deletion syndrome, which only has six reported cases, encompasses this gene and shares cryptorchidism, pylectasis/hydronephrosis, developmental delay, and various neurologic malformations including hypoplasia of the corpus callosum.[23] Last, while none of these variants were present in gnomAD, of the 59.8 expected LoF variants, only three have been observed, and two of those have been flagged for further review on quality or annotation. This produces an observed over expected ratio of 0.05 and is within the range associated with genes intolerant to LoF. The remaining individual in gnomAD would need an evaluation because both the milder neurologic and urogenital phenotypic spectrum may not be apparent without further clinical examination.

The pathogenesis of brain malformations secondary to haploinsufficiency of *PPP1R12A* is incompletely understood. Experiments have shown that elimination of either MP subunit (PPP1R12A or PP1c) results in lost expression of the remaining subunit and is thought to contribute to decreased activity of the MP holoenzyme.[24] We show here that *Ppp1r12a* is expressed in the neural folds of the embryonic mouse brain at the critical time for forebrain development (Figure 2). Forebrain division occurs in early embryogenesis. A complex signaling pattern, including sonic hedgehog, emanates from the prechordal plate (PrCP) beneath the telencephalon and directs median forebrain expansion and division shortly after gastrulation.[25] Brain malformations including HPE, anencephaly, and agenesis of the corpus callosum were found in these individuals. HPE occurs in approximately one in 10,000 liveborns and one in 250 conceptuses. The clinical spectrum of HPE ranges from the most severe form with cyclopia and one cerebral ventricle (alobar HPE) to almost complete cerebral hemisphere division (lobar HPE). The etiology of HPE is heterogenous, and both genetic and environmental causes have been identified. However, most individuals with unremarkable karyotypes remain undiagnosed.[26,27] Individuals 1 and 2 had HPE which precisely matched the cyclopia phenotype in zebrafish; the most severe finding was fetal acrania with exencephaly seen in individual 4. The pathways associated with HPE are perturbed in human and animal models of exencephaly; these pathways include *Tgif* (mouse model), *Shh,* and *Gli2*,[28] and

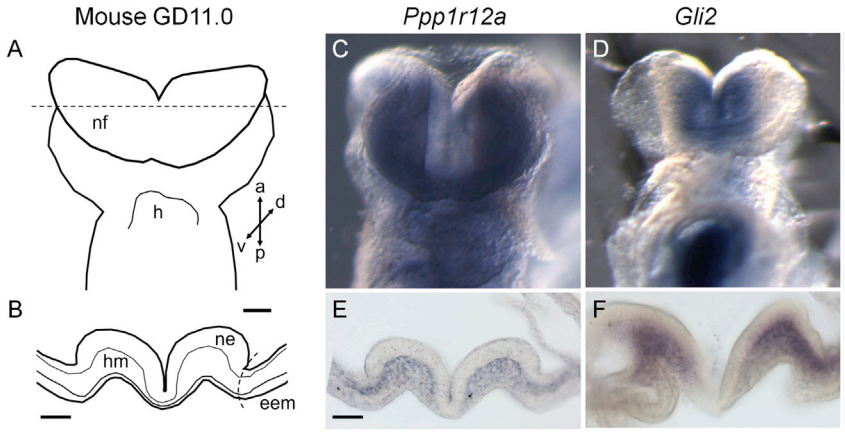

Figure 2. Brain: Mouse *in situ* Hybridization of the Prosencephalic Neural Folds
Gestational day 8.25 mouse embryos were stained via *in situ* hybridization in order to determine gene expression patterns. A ventral view is shown for whole mounts. Transverse sections through the prosencephalic neural folds (at the level of the dashed line in schematic) were stained in order to visualize gene expression in specific cellular compartments. *Ppp1r12a* localized to the head mesenchyme and is absent from extra-embryonic membranes. nf—neural folds, h—heart, ne—neuroectoderm, hm—head mesenchyme, eem—extra-embryonic membranes. Scale bar = 100 μm.

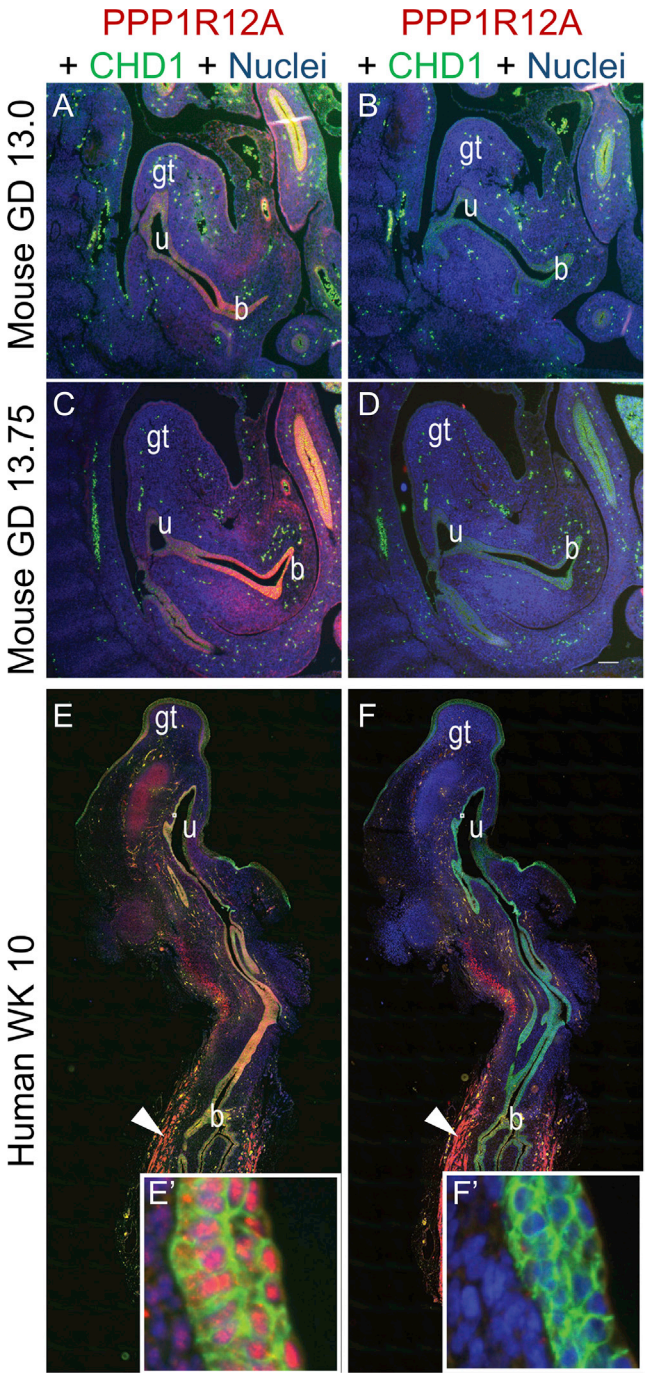

Figure 3. Urogenital: Mouse and Human Immunostaining of the Genitourinary Tract

(A–B) Tissue sections from mouse genitourinary tracts at gestation day (GD) 13.

(C–D) Mouse genitourinary tracts at GD13.75.

(E–F) Human genitourinary tracts at week 10 were immunostained in order to detect protein localization patterns. PPP1R12A was detected in genital tubercle epithelium (ectoderm derived), bladder, and urethral epithelium (endoderm derived), and a subset or urogenital sinus mesenchymal cells (arrowhead) bladder detrusor smooth muscle. (E′) PPP1R12A localized to epithelial cell nuclei of human urethra (lower image, inset). (F′, arrowhead) PPP1R12B detected in developing human detrusor smooth muscle (B, D, F, F′) but not in developing mouse or human bladder or urogenital sinus epithelial cells. Abbreviations are B—bladder, GT—genital tubercle, U—urethra.

13q deletions which include *ZIC2* (humans). Additionally, in a series of 150 embryos with HPE, 14 were noted to have exencephaly and/or myeloschisis.[29] Gathering more individuals with fetal acrania may provide another area to investigate for variants in *PPP1R12A*.

While these individuals provide initial evidence supporting the importance of *PPP1R12A* in development, more research will be needed in order to understand the precise mechanism that *PPP1R12A* causes in these malformations. Current evidence does not support the possibility that *PPP1R12A* is part of the canonical pathways of HPE such as the hedgehog signaling pathways; however, *PPP1R12A* has an established role in cell migration, cell adhesion, and cytoskeletal organization.[30,31] Animal models, such as zebrafish morpholino knockdown of ppp1r12a (also known as mypt), resulted in defective PrCP anterior migration,[12] and removal of the PrCP resulted in cyclopia.[32–34] These findings support the association between *PPP1R12A* LoF variants and HPE. While the zebrafish provides a commonly used model for comparison to human neurodevelopment, due to its less-understood mechanisms, it does not model human sex differentiation and gonadal development.[35] As seen with the zebrafish, we draw connections between the cell migration defects and midline brain malformations.

Other genetic conditions known to have both brain and urogenital malformations include Smith-Lemli-Opitz syndrome (MIM: 270400), X-linked lissencephaly (MIM: 300215), microcephaly, facial dysmorphism, renal agenesis, and ambiguous genitalia syndrome (MIM: 618142), pontocerebellar hypoplasia type 7 (MIM: 614969), orofaciodigital syndrome IV (MIM: 258860), and other conditions with complete gonadal dysgenesis and discordance between the phenotypic and genotypic sex. Syndromic and non-syndromic causes have also been reported, but the etiology in many affected individuals remains broad due to the phenotypic overlap between individuals with partial androgen insensitivity and those with partial gonadal dysgenesis.[36–38] Individuals 5–12 had a wide spectrum of genitourinary phenotypes from partial gonadal dysgenesis with micropenis, hypospadias, and ambiguous genitals with Müllerian duct remnants to complete gonadal dysgenesis in a genotypic 46,XY individual with female external genitalia. *Ppp1r12a* has been noted to be increased in mouse striated and smooth muscle during sexual differentiation with higher levels in males than females.[39] The high number of 46,XY individuals with urogenital anomalies (nine out of 12) in this report may either reflect ascertainment bias or a probable sex-influenced mechanism, in contrast to the remaining three 46,XX individuals with severe brain anomalies (HPE and anencephaly).

Müllerian ducts are formed via several steps including specification, invagination through apical constriction, and elongation. Multiple signaling systems are involved in the process of Müllerian duct formation; these include RhoA GTPases, molecules known to modulate

the processes of many epithelial tissue invaginations and morphogenesis through the indirect increase of non-muscle myosin II activity. Given the clinical findings, we propose that alterations to this pathway could change the development of these ducts and subsequently lead to defective regression of the Müllerian ducts, in the presence of sex-determining region Y (SRY), and ultimately result in a DSD. Sexual differentiation occurs in the undifferentiated zygote through complex interactions between genetic and developmental processes. During this process, phenotypical sexual differences are evolved through the presence or absence of SRY and through impairment of the cascades of developmental events downstream. However, the developmental processes that cause DSD remain unknown, and in many instances, individuals do not receive a molecular diagnosis. Recently, the Rho-kinase pathway was found to be a major regulator of the male urogenital function and disorders.[40] Notably, PPP1R12A, which is downstream of this system, is highly localized in the developing reproductive system[39] and remains highly expressed in human adult uterus and vagina (GTEx). While the specific role of *PPP1R12A* in external and internal genitalia development has not been previously described, these individuals provide a starting point for further research regarding the role of this gene in DSD.

In summary, these 12 individuals illustrate the association of *PPP1R12A* with HPE spectrum phenotypes and urogenital malformations including DSD. *In situ* mouse hybridization studies of *Ppp1r12a* demonstrate expression precisely at the proper time and location for brain development implicated in HPE, and our immunostaining of PPP1R12A in the mouse embryo and human tissue reveals protein localization patterns in the developing lower urinary tract epithelium, which is responsible for bladder, urethral, and genital tubercle formation.

Accession Numbers

The accession number for the sequence reported in this paper is ClinVar: VCV000450254.

Supplemental Data

Supplemental Data can be found online at https://doi.org/10.1016/j.ajhg.2019.12.004.

Acknowledgments

We thank the families for their participation in this publication. This work was supported by the National Human Genome Research Institute Intramural Research program. Work in the R.J.L. lab was supported by the National Institute of Environmental Health Sciences of the National Institutes of Health (NIH) under award numbers R01ES026819 and T32ES007015. Work in the CMV lab was supported by NIH grant U01DK110807. E.D., E.V., M.R., and P.F. are supported in part by the Disorder of Sex Development Translational Research Network (R01 HD093450). The DSD whole-genome sequencing project was funded by the Gabriella Miller Kids First Initiative (XO1HL132384, E.V.). We are grateful for the help of Linda Ramsdell, MS, CGC (Seattle Children's Hospital) and Kimberly Kennedy, RN (Cincinnati Children's Hospital) for individuals 11 and 12. The Genotype-Tissue Expression (GTEx) Project was supported by the Common Fund of the Office of the Director of the NIH, and by the National Cancer Institute (NCI), the National Human Genome Research Institute (NHGRI), the National Heart, Lung, and Blood Institute (NHLBI), the National Institute on Drug Abuse (NIDA), the National Institute of Mental Health (NIMH), and the National Institute of Neurological Disorders and Stroke (NINDS). The data used for the analyses described in this manuscript were obtained from the GTEx Portal on 10/10/19.

Declaration of Interests

The authors declare no competing interests.

Received: October 21, 2019
Accepted: December 4, 2019
Published: December 26, 2019

Web Resources

DECIPHER, https://decipher.sanger.ac.uk/
gnomAD, https://gnomad.broadinstitute.org/
GTEx, https://gtexportal.org/home/
OMIM, https://omim.org/
UniProt, https://uniprot.org/

References

1. Grassie, M.E., Moffat, L.D., Walsh, M.P., and MacDonald, J.A. (2011). The myosin phosphatase targeting protein (MYPT) family: a regulated mechanism for achieving substrate specificity of the catalytic subunit of protein phosphatase type 1δ. Arch. Biochem. Biophys. *510*, 147–159.
2. Kiss, A., Erdődi, F., and Lontay, B. (2019). Myosin phosphatase: Unexpected functions of a long-known enzyme. Biochim. Biophys. Acta Mol. Cell Res. *1866*, 2–15.
3. Ito, M., Nakano, T., Erdodi, F., and Hartshorne, D.J. (2004). Myosin phosphatase: structure, regulation and function. Mol. Cell. Biochem. *259*, 197–209.
4. Shichi, D., Arimura, T., Ishikawa, T., and Kimura, A. (2010). Heart-specific small subunit of myosin light chain phosphatase activates rho-associated kinase and regulates phosphorylation of myosin phosphatase target subunit 1. J. Biol. Chem. *285*, 33680–33690.
5. Shimizu, H., Ito, M., Miyahara, M., Ichikawa, K., Okubo, S., Konishi, T., Naka, M., Tanaka, T., Hirano, K., Hartshorne, D.J., et al. (1994). Characterization of the myosin-binding subunit of smooth muscle myosin phosphatase. J. Biol. Chem. *269*, 30407–30411.
6. Huang, H., Ruan, H., Aw, M.Y., Hussain, A., Guo, L., Gao, C., Qian, F., Leung, T., Song, H., Kimelman, D., et al. (2008). Mypt1-mediated spatial positioning of Bmp2-producing cells is essential for liver organogenesis. Development *135*, 3209–3218.
7. Alessi, D., MacDougall, L.K., Sola, M.M., Ikebe, M., and Cohen, P. (1992). The control of protein phosphatase-1 by targetting subunits. The major myosin phosphatase in avian

smooth muscle is a novel form of protein phosphatase-1. Eur. J. Biochem. *210*, 1023–1035.
8. Tan, C., Stronach, B., and Perrimon, N. (2003). Roles of myosin phosphatase during Drosophila development. Development *130*, 671–681.
9. Mizuno, T., Tsutsui, K., and Nishida, Y. (2002). Drosophila myosin phosphatase and its role in dorsal closure. Development *129*, 1215–1223.
10. Wissmann, A., Ingles, J., and Mains, P.E. (1999). The Caenorhabditis elegans mel-11 myosin phosphatase regulatory subunit affects tissue contraction in the somatic gonad and the embryonic epidermis and genetically interacts with the Rac signaling pathway. Dev. Biol. *209*, 111–127.
11. Okamoto, R., Ito, M., Suzuki, N., Kongo, M., Moriki, N., Saito, H., Tsumura, H., Imanaka-Yoshida, K., Kimura, K., Mizoguchi, A., et al. (2005). The targeted disruption of the MYPT1 gene results in embryonic lethality. Transgenic Res. *14*, 337–340.
12. Weiser, D.C., Row, R.H., and Kimelman, D. (2009). Rho-regulated myosin phosphatase establishes the level of protrusive activity required for cell movements during zebrafish gastrulation. Development *136*, 2375–2384.
13. Kruszka, P., Berger, S.I., Casa, V., Dekker, M.R., Gaesser, J., Weiss, K., Martinez, A.F., Murdock, D.R., Louie, R.J., Prijoles, E.J., et al. (2019). Cohesin complex-associated holoprosencephaly. Brain *142*, 2631–2643.
14. Sobreira, N., Schiettecatte, F., Valle, D., and Hamosh, A. (2015). GeneMatcher: a matching tool for connecting investigators with an interest in the same gene. Hum. Mutat. *36*, 928–930.
15. Ren, J., Wen, L., Gao, X., Jin, C., Xue, Y., and Yao, X. (2009). DOG 1.0: illustrator of protein domain structures. Cell Res. *19*, 271–273.
16. Chiang, C., Litingtung, Y., Lee, E., Young, K.E., Corden, J.L., Westphal, H., and Beachy, P.A. (1996). Cyclopia and defective axial patterning in mice lacking Sonic hedgehog gene function. Nature *383*, 407–413.
17. Hong, S., Hu, P., Marino, J., Hufnagel, S.B., Hopkin, R.J., Toromanović, A., Richieri-Costa, A., Ribeiro-Bicudo, L.A., Kruszka, P., Roessler, E., and Muenke, M. (2016). Dominant-negative kinase domain mutations in FGFR1 can explain the clinical severity of Hartsfield syndrome. Hum. Mol. Genet. *25*, 1912–1922.
18. Solomon, B.D., Bear, K.A., Wyllie, A., Keaton, A.A., Dubourg, C., David, V., Mercier, S., Odent, S., Hehr, U., Paulussen, A., et al. (2012). Genotypic and phenotypic analysis of 396 individuals with mutations in Sonic Hedgehog. J. Med. Genet. *49*, 473–479.
19. Heyne, G.W., Everson, J.L., Ansen-Wilson, L.J., Melberg, C.G., Fink, D.M., Parins, K.F., Doroodchi, P., Ulschmid, C.M., and Lipinski, R.J. (2016). Gli2 gene-environment interactions contribute to the etiological complexity of holoprosencephaly: evidence from a mouse model. Dis. Model. Mech. *9*, 1307–1315.
20. Lewis, B.P., Green, R.E., and Brenner, S.E. (2003). Evidence for the widespread coupling of alternative splicing and nonsense-mediated mRNA decay in humans. Proc. Natl. Acad. Sci. USA *100*, 189–192.
21. Chang, Y.F., Imam, J.S., and Wilkinson, M.F. (2007). The nonsense-mediated decay RNA surveillance pathway. Annu. Rev. Biochem. *76*, 51–74.
22. Szabo, L., Morey, R., Palpant, N.J., Wang, P.L., Afari, N., Jiang, C., Parast, M.M., Murry, C.E., Laurent, L.C., and Salzman, J. (2015). Statistically based splicing detection reveals neural enrichment and tissue-specific induction of circular RNA during human fetal development. Genome Biol. *16*, 126.
23. McKenna, C.S., Saxena, N., Dabir, T.A., Jones, J., Smith, G., and Morrison, P.J. (2019). Phenotypic delineation of a 12q21 deletion syndrome. Clin. Dysmorphol. *28*, 198–201.
24. Scotto-Lavino, E., Garcia-Diaz, M., Du, G., and Frohman, M.A. (2010). Basis for the isoform-specific interaction of myosin phosphatase subunits protein phosphatase 1c beta and myosin phosphatase targeting subunit 1. J. Biol. Chem. *285*, 6419–6424.
25. Roessler, E., and Muenke, M. (2010). The molecular genetics of holoprosencephaly. Am. J. Med. Genet. C. Semin. Med. Genet. *154C*, 52–61.
26. Kruszka, P., Martinez, A.F., and Muenke, M. (2018). Molecular testing in holoprosencephaly. Am. J. Med. Genet. C. Semin. Med. Genet. *178*, 187–193.
27. Kruszka, P., and Muenke, M. (2018). Syndromes associated with holoprosencephaly. Am. J. Med. Genet. C. Semin. Med. Genet. *178*, 229–237.
28. Kietzman, H.W., Everson, J.L., Sulik, K.K., and Lipinski, R.J. (2014). The teratogenic effects of prenatal ethanol exposure are exacerbated by Sonic Hedgehog or GLI2 haploinsufficiency in the mouse. PLoS ONE *9*, e89448.
29. Cohen, M.M., Jr. (2006). Holoprosencephaly: clinical, anatomic, and molecular dimensions. Birth Defects Res. A Clin. Mol. Teratol. *76*, 658–673.
30. Xia, D., Stull, J.T., and Kamm, K.E. (2005). Myosin phosphatase targeting subunit 1 affects cell migration by regulating myosin phosphorylation and actin assembly. Exp. Cell Res. *304*, 506–517.
31. Zagórska, A., Deak, M., Campbell, D.G., Banerjee, S., Hirano, M., Aizawa, S., Prescott, A.R., and Alessi, D.R. (2010). New roles for the LKB1-NUAK pathway in controlling myosin phosphatase complexes and cell adhesion. Sci. Signal. *3*, ra25.
32. Feldman, B., Gates, M.A., Egan, E.S., Dougan, S.T., Rennebeck, G., Sirotkin, H.I., Schier, A.F., and Talbot, W.S. (1998). Zebrafish organizer development and germ-layer formation require nodal-related signals. Nature *395*, 181–185.
33. Schier, A.F. (2003). Nodal signaling in vertebrate development. Annu. Rev. Cell Dev. Biol. *19*, 589–621.
34. Shih, J., and Fraser, S.E. (1996). Characterizing the zebrafish organizer: microsurgical analysis at the early-shield stage. Development *122*, 1313–1322.
35. Santos, D., Luzio, A., and Coimbra, A.M. (2017). Zebrafish sex differentiation and gonad development: A review on the impact of environmental factors. Aquat. Toxicol. *191*, 141–163.
36. Délot, E.C., Papp, J.C., Sandberg, D.E., Vilain, E.; and DSD-TRN Genetics Workgroup (2017). Genetics of Disorders of Sex Development: The DSD-TRN Experience. Endocrinol. Metab. Clin. North Am. *46*, 519–537.
37. Parivesh, A., Barseghyan, H., Délot, E., and Vilain, E. (2019). Translating genomics to the clinical diagnosis of disorders/differences of sex development. Curr. Top. Dev. Biol. *134*, 317–375.
38. Délot, E.C., and Vilain, E.J. (2003 Oct 30). Nonsyndromic 46,XX Testicular Disorders of Sex Development. In

GeneReviews, M.P. Adam, H.H. Ardinger, R.A. Pagon, S.E. Wallace, L.J.H. Bean, K. Stephens, and A. Amemiya, eds. (Seattle: University of Washington), pp. 1993–2019, [Internet].

39. Lontay, B., Bodoor, K., Weitzel, D.H., Loiselle, D., Fortner, C., Lengyel, S., Zheng, D., Devente, J., Hickner, R., and Haystead, T.A. (2010). Smoothelin-like 1 protein regulates myosin phosphatase-targeting subunit 1 expression during sexual development and pregnancy. J. Biol. Chem. *285*, 29357–29366.

40. Gur, S., Kadowitz, P.J., and Hellstrom, W.J. (2011). RhoA/Rho-kinase as a therapeutic target for the male urogenital tract. J. Sex. Med. *8*, 675–687.

The American Journal of Human Genetics, Volume *106*

Supplemental Data

Loss-of-Function Variants in *PPP1R12A*: From Isolated Sex Reversal to Holoprosencephaly Spectrum and Urogenital Malformations

Joel J. Hughes, Ebba Alkhunaizi, Paul Kruszka, Louise C. Pyle, Dorothy K. Grange, Seth I. Berger, Katelyn K. Payne, Diane Masser-Frye, Tommy Hu, Michelle R. Christie, Nancy J. Clegg, Joshua L. Everson, Ariel F. Martinez, Laurence E. Walsh, Emma Bedoukian, Marilyn C. Jones, Catharine Jean Harris, Korbinian M. Riedhammer, Daniela Choukair, Patricia Y. Fechner, Meilan M. Rutter, Sophia B. Hufnagel, Maian Roifman, Gad B. Kletter, Emmanuele Delot, Eric Vilain, Robert J. Lipinski, Chad M. Vezina, Maximilian Muenke, and David Chitayat

Supplemental Note: Case Reports

Individual 1: She was born at term to a 19-year-old mother by Cesarean delivery and weighed 3.23 kg (50^{th} centile). The pregnancy was complicated by maternal hypertension, pre-eclampsia, diabetes, and exposure to alcohol and marijuana at approximately 8 weeks gestation. She had syntelencephaly/middle interhemispheric variant (MIHV) of HPE, polymicrogyria, and Chiari I malformation identified on brain MRI. Other medical problems included intellectual disability, attention deficit hyperactivity disorder (ADHD), and seizures. Sanger sequencing of the four most common genes associated with HPE, *SHH* (MIM: 600725), *ZIC2* (MIM: 603073), *SIX3* (MIM: 603714), and *TGIF* (MIM: 602630), failed to identify any detectable pathogenic variants. Trio exome sequencing revealed a heterozygous *de novo* variant in *PPP1R12A,* NM_002480.3:c.2033_2034del p.(Ser678*), which was confirmed by Sanger sequencing.

Individual 2: She was a 6-year-old female with semilobar HPE and agenesis of the corpus callosum identified on MRI. Other medical problems included myoclonus, intellectual disability, and syndactyly of the toes. Sanger sequencing of *SHH, SIX3, ZIC2,* and *TGIF* failed to identify detectable pathogenic variants. Trio exome sequencing revealed a heterozygous *de novo* variant in *PPP1R12A,* NM_002480.3:c.1415C>G p.(Ser472*), which was confirmed by Sanger sequencing.

Individual 3: Prenatally, he had a fetal ultrasound and MRI which demonstrated agenesis of the corpus callosum and colpocephaly as well as pyelectasis and intrauterine growth restriction. Chromosome analysis of amniocytes showed 46,XY Normal male. A Cesarean delivery occurred at 36 2/7 weeks for breech presentation and oligohydramnios. Significant findings on newborn evaluation included low birth weight of 2.04 kg (3-10^{th} centile), decreased subcutaneous fat, mild facial asymmetry, ulnar drift at the wrist and fisting, upper back kyphosis, and grade 1 hydronephrosis with renal asymmetry detected by ultrasound. Findings at age 5.5 years were grossly unchanged apart from additional behavioral issues including ADHD and defiance. A chromosome microarray analysis (CMA) was arr(1-22normal. Trio

exome sequencing through GeneDx revealed a heterozygous *de novo* splice site variant in *PPP1R12A,* NM_002480.3: c.793-1G>A.

Individual 4: Prenatally, an 11-week antenatal ultrasound showed fetal acrania with exencephaly, hypertelorism, flattened facial profile with non-visualization of the nasal bone, omphalocele, echogenic bowel, and non-visualization of the lumbosacral spine. Fetal growth was normal. The parents were of Chinese descent, non-consanguineous and with an unremarkable family history. The pregnancy was interrupted and limited pathological assessment of the fetus and placenta at 12 weeks gestation revealed the presence of a partial cranial vault with scant white-grey tissue and spinal column. Chorionic villus and fetal neural, renal, gastrointestinal, and cardiac tissues were histologically examined and unremarkable. Maternal serum folate and vitamin B12 levels were within normal range. CMA on products of conception was arr(1-22,X)x2 normal female. *UPD11* testing and *CDKN1C* sequencing obtained due to the presence of an omphalocele on ultrasound showed no abnormalities. Trio exome sequencing identified a heterozygous *de novo* frameshift variant in *PPP1R12A,* NM_002480.3:c.223_224delAC p.(Thr75Cysfs*8).

Individual 5: He was a 3-year-old male with ambiguous genitalia at birth. Physical exam revealed micropenis, chordee, scrotal hypospadias, bilateral cryptorchidism, and a uterus on ultrasound. No other birth defects were reported. Additionally, serum anti-Müllerian hormone levels were below normal range. Karyotype was 46,XY Normal male. Developmentally, he was reported appropriate for age and had an unremarkable head CT scan. Trio exome sequencing by GeneDx identified a *de novo* heterozygous frameshift variant in *PPP1R12A* NM_002480.3: c.2739_2740delCT p.(Leu914Argfs*14).

Individual 6: He was a 6-year-old male found on fetal ultrasound, at 19 weeks of gestation, to have an encephalocele at the posterior parietal region and colpocephaly. The pregnancy was complicated by chronic maternal hypertension, type II diabetes mellitus controlled with insulin, and intrauterine growth restriction. At birth, he was noted to have thrombocytopenia requiring platelet transfusion. He had ventriculoperitoneal shunt insertion for hydrocephalus and encephalocele repair shortly after birth. Postnatal MRI revealed dysgenesis of the corpus callosum, absent septum pellucidum, Chiari

malformation, cortical dysplasia/polymicrogyria and grey matter heterotopia. Neurological examination was notable for global developmental delay, intellectual disability, autistic features, appendicular hypotonia with foot pronation requiring supra malleolar orthosis (SMO) braces bilaterally, and an unsteady gait. He sat at 1 year, walked at 3 years, and continued to have difficulties with expressive language with limited speech. He had minor dysmorphic facial features including short upslanting palpebral fissures, low-set ears, and micrognathia. Other significant features included short stature, patent ductus arteriosus, and ophthalmologic abnormalities including strabismus, astigmatism, hyperopia, and alternating esotropia. The genitourinary abnormalities included glandular hypospadias and chordee which required surgical correction. Karyotype was 46,XY Normal male and trio exome sequencing by GeneDx identified a heterozygous nonsense *de novo* variant in *PPP1R12A* NM_002480.3:c.1510C>T p.(Arg504*).

Individual **7:** He was a 7-year-old male with genitourinary malformations including hypospadias, cryptorchidism, and a uterus. The prenatal and early medical history is unknown, as he was adopted out. Karyotype was 46,XY Normal male. He had generalized developmental delay, seizures and brain MRI showed microcephaly and leukomalacia along with opacified left tympanic cavity and mastoid air cells. Facial dysmorphism was noted including long face, large prominent ears, ptosis, and a small pointed nose. Other abnormalities included, 5th finger clinodactyly, and blind shallow rectal cleft. Further investigation revealed delayed bone age, bilateral rod and cone dysfunction with decreased vision, and latent nystagmus. Singleton exome sequencing by GeneDx revealed a heterozygous nonsense variant in *PPP1R12A,* NM_002480.3:c.2573G>A p.(Trp858*).

Individual 8**:** She was a 45-year-old female with typical female external genitalia and a 46,XY Normal male karyotype. Pelvic ultrasound identified a small uterus didelphys. She had a history of a bilateral gonadectomy in childhood; however, the pathologist did not specify ovarian or testicular tissue on report. She had primary amenorrhea and was over 6 feet tall. *SRY* and *NR5A1* gene sequencing were unremarkable. There were no reported neurological issues, developmental delay, or other malformations.

Singleton exome sequencing performed at GeneDx identified a heterozygous frameshift in *PPP1R12A* NM_002480.3:c.2073dupA p.(Ser692Ilefs*2).

Individual 9: She was a 9-month-old phenotypic female with a 46,XY Normal male karyotype, and had external genitalia notable for clitoral hypertrophy (0.5 cm in diameter), urogenital sinus (UGS), vaginal opening and posterior fusion of the labia majora. No uterus was identified on pelvic ultrasound. Prenatal history was unremarkable with spontaneous vaginal delivery at 39 weeks. Biochemical workup was not consistent with congenital adrenal hyperplasia. Neuroimaging was not indicated at that time. Trio exome sequencing performed via a German health care project for rare diseases revealed a heterozygous *de novo* nonsense variant in *PPP1R12A* NM_002480.3:c.2698C>T p.(Arg900*).

Individual 10: He was a 2-year-old phenotypic male with 46,XY Normal male karyotype, evaluated by clinical genetics due to grade 2 hypospadias and cryptorchidism. He was born premature at 27 weeks. A Fallopian tube without mention of an attached gonad was identified during surgical repair of a right inguinal hernia. Abdominal ultrasound showed a uterus. Physical exam was notable for short stature, macrocephaly, triangular face, long palpebral fissures, ptosis, small mouth and wide nasal tip. He had global developmental delay and brain MRI was normal. A CMA was normal. Trio exome sequencing by GeneDx revealed a likely pathogenic heterozygous maternally inherited variant in *SCN8A,* NM_01491.3:c.2424dupT p.(Pro809Serfs*13) which was identified in a clinically unaffected sib, as well as a heterozygous *de* novo variant in *PPP1R12A,* NM_002480.3:c.960dupA p.(Glu321Argfs*6).

Individual 11**:** She was a adult female with 46,XY gonadal dysgenesis, alopecia totalis, obesity and acanthosis nigricans. Diagnostic laparoscopy at age 6 identified two streak gonads (abdominal on the right and inguinal on the left) which were resected, with rudimentary Fallopian tubes, a vaginal opening, and no uterus. She has had normal development and brain MRI was normal. At age 30, she is doing well on hormone replacement therapy. Trio research genome sequencing identified a heterozygous *de novo* variant in *PPP1R12A*, NM_002480.3:c.1189delA p.(Thr397Hisfs*42) which was confirmed by Sanger sequencing.

Individual 12: She was evaluated by genetics due to discordance between the chromosome sex (46,XY) on cell free non-invasive prenatal testing and the phenotypic sex as identified on fetal ultrasound showing a female external genitalia. Postnatally, she was noted to have jejunal and ileal atresia. Surgery revealed an aberrant mesenteric blood supply, normal-appearing ovaries with Fallopian tubes and a uterus. CMA was arr(1-22)x2,(X,Y)x1 normal male. An ultrasound at 1 year showed normal kidneys and confirmed the presence of a uterus, but did not identify gonads, suggesting gonadal degeneration. Examination at age 2 showed a clitoris, posterior labial fusion, increased labial rugation and pigmentation, and mild gynecomastia. Her growth parameters were normal. She had strabismus, bilateral epicanthus inversus, right esotropia, abnormal auricles, bilateral 5th digit clinodactyly, and spoon-shaped toenails. She had developmental delay and autism spectrum disorder. Brain MRI has not been done. Luteinizing hormone and FSH was within normal range, and anti-müllerian hormone and testosterone was lower than normal range for a male with a 46,XY karyotype. Research genome sequencing identified a heterozygous *de novo* variant in *PPP1R12A*, NM_002480.3:c.681dupT (p.Lys228Ter) which was confirmed by Sanger sequencing.

Supplemental Material and Methods

Brain: mouse *in situ* hybridization. Genes that regulate forebrain patterning and play a role in HPE pathogenesis are expected to be expressed in the prosencephalic neural folds that give rise to the forebrain during primary neurulation.[1] Therefore, we conducted *in situ* hybridization (ISH) on mouse embryos at gestational day (GD) 8.25. This stage is representative of early neurulation and within the critical period for development of HPE.[2, 3] Studies were conducted in strict accordance with the recommendations in the *Guide for the Care and Use of Laboratory Animals* of the National Institutes of Health. The protocol was approved by the University of Wisconsin-Madison School of Veterinary Medicine Institutional Animal Care and Use Committee (protocol

number G005396). CD-1 mice (Mus musculus) were purchased from Charles River and C57BL/6J mice from The Jackson Laboratory. Timed-pregnancies were established as previously described.[4] Embryos were dissected at GD8.25 and fixed overnight in 4% paraformaldehyde. *In situ* hybridization (ISH) was conducted on whole C57BL/6J embryos or 50 µm sections cut from CD-1 embryos with a vibrating microtome in the transverse plane along the anterior-posterior axis. ISH was conducted as previously described.[5]

Urogenital: mouse and human immunostaining. Human lower urinary tracts were obtained from the Joint MRC / Wellcome (MR/R006237/1) Human Developmental Biology Resource (www.hdbr.org) under an approved University of Wisconsin-Madison IRB protocol (2016-0449). C57BL/6J mouse lower urinary tracts were obtained under a University of Wisconsin-Madison approved ACUC protocol (protocol number G005396). Tissues were embedded in paraffin and stained with antibodies against PPP1R12A (Thermo Scientific PA579857, 1:250), PPP1R12B (Sigma HPA024171, 1:250), CDH1 (BD Transduction Labs 610181, 1:250) and with DAPI (nuclei) using an established method.[6] Mouse results are representative of three independent mice per group and human results are representative of one per group.

DNA Sequence and Analysis Methods

National Institutes of Health: DNA samples from study participants underwent exome sequencing at the National Intramural Sequencing Center (NISC) as previously described.[7] The mean read depth for each sample was 79.8. Copy number variation (CNV) prediction from exome data was done using the XHMM (eXome-Hidden Markov Model) caller.[8] We used

GATK to generate the depth of coverage statistics required for XHMM from the BAM files of our HPE cohort and a control set. GATK output was then run through the XHMM pipeline, generating a VCF file containing each predicted CNV. We then annotated each CNV for genes contained and cytogenetic region using Annovar. All probands were first searched for four common genes known to cause HPE: *SHH* (MIM: 600725) on 7q36, *ZIC2* (MIM: 603073) on 13q32, *SIX3* (MIM: 603714) on 2p21, and *TGIF* (MIM: 602630) on 18p11.3 using Sanger sequencing as recommended.[9] With the goal of new gene discovery, minimizing false positives, and sacrificing sensitivity, the discovery cohort was filtered with stringent criteria including *de novo* inheritance in genes intolerant of variation,[10] variant absence in the ExAC database,[10] and Combined Annotation-Dependent Depletion (CADD) scores above 20.[11] Variants that met these criteria were considered deleterious. A total of 101 trios affected by holoprosencephaly (proband, father, and mother) were sequenced.

Technical University of Munich: DNA was extracted from peripheral blood using the Gentra Puregene Blood Kit (Qiagen, Hilden, Germany) according to the manufacturer's instructions. Trio exome sequencing (ES) was performed using a Sure Select Human All Exon 60 Mb V6 Kit (Agilent) and a NovaSeq 6000 (Illumina) as previously described.[12] Mitchondrial DNA was derived from off-target exome reads as previously described.[13] Reads were aligned to the human reference genome (UCSC Genome Browser build hg19) using Burrows-Wheeler Aligner (v.0.7.5a). Detection of single-nucleotide variants and small insertions and deletions (indels) was performed with SAMtools (version 0.1.19). ExomeDepth was used for the detection of copy number variations (CNVs).[14] For the analysis of *de novo,* autosomal dominant and mitochondrial variants, only variants with a minor allele frequency (MAF) of less than 0.1% in the in-house

database of the Helmholtz center Munich containing over 18,000 exomes were considered. For the analysis of autosomal recessive and X-linked variants (homozygous, hemizygous or compound heterozygous) only variants with a MAF of less than 1.0% were considered.

Children's National Hospital: A cohort of 300 samples, belonging to 94 families with a variety of syndromic or isolated DSD conditions was sequenced. Whole genome sequencing at an average 30x coverage was performed on a HiSeqX instrument at the Baylor facility under the Gabriella Miller Kids First Initiative XO1 mechanism (https://commonfund.nih.gov/kidsfirst/x01projects). Targeted search for exonic variants in *PPP1R12A* analysis was performed using both the Genoox platform (https://www.genoox.com/) and the Broad Institute's *Seqr* software (https://www.seqr.broadinstitute.org/).

GeneDx: Limited availability of detailed commercial practices regarding exome processing and analysis. Test info sheet for XomeDx accessible through their public website for review (https://www.genedx.com/).

Supplemental References

1. Geng, X., and Oliver, G. (2009). Pathogenesis of holoprosencephaly. J Clin Invest 119, 1403-1413.
2. Heyne, G.W., Melberg, C.G., Doroodchi, P., Parins, K.F., Kietzman, H.W., Everson, J.L., Ansen-Wilson, L.J., and Lipinski, R.J. (2015). Definition of critical periods for Hedgehog

pathway antagonist-induced holoprosencephaly, cleft lip, and cleft palate. PLoS One 10, e0120517.

3. Heyne, G.W., Everson, J.L., Ansen-Wilson, L.J., Melberg, C.G., Fink, D.M., Parins, K.F., Doroodchi, P., Ulschmid, C.M., and Lipinski, R.J. (2016). Gli2 gene-environment interactions contribute to the etiological complexity of holoprosencephaly: evidence from a mouse model. Dis Model Mech 9, 1307-1315.

4. Heyne, G.W., Plisch, E.H., Melberg, C.G., Sandgren, E.P., Peter, J.A., and Lipinski, R.J. (2015). A Simple and Reliable Method for Early Pregnancy Detection in Inbred Mice. J Am Assoc Lab Anim Sci 54, 368-371.

5. Everson, J.L., Fink, D.M., Yoon, J.W., Leslie, E.J., Kietzman, H.W., Ansen-Wilson, L.J., Chung, H.M., Walterhouse, D.O., Marazita, M.L., and Lipinski, R.J. (2017). Sonic hedgehog regulation of Foxf2 promotes cranial neural crest mesenchyme proliferation and is disrupted in cleft lip morphogenesis. Development 144, 2082-2091.

6. Abler, L.L., Keil, K.P., Mehta, V., Joshi, P.S., Schmitz, C.T., and Vezina, C.M. (2011). A high-resolution molecular atlas of the fetal mouse lower urogenital tract. Dev Dyn 240, 2364-2377.

7. Kruszka, P., Uwineza, A., Mutesa, L., Martinez, A.F., Abe, Y., Zackai, E.H., Ganetzky, R., Chung, B., Stevenson, R.E., Adelstein, R.S., et al. (2015). Limb body wall complex, amniotic band sequence, or new syndrome caused by mutation in IQ Motif containing K (IQCK)? Mol Genet Genomic Med 3, 424-432.

8. Fromer, M., Moran, J.L., Chambert, K., Banks, E., Bergen, S.E., Ruderfer, D.M., Handsaker, R.E., McCarroll, S.A., O'Donovan, M.C., Owen, M.J., et al. (2012). Discovery and statistical

genotyping of copy-number variation from whole-exome sequencing depth. Am J Hum Genet 91, 597-607.

9. Kruszka, P., Martinez, A.F., and Muenke, M. (2018). Molecular testing in holoprosencephaly. Am J Med Genet C Semin Med Genet 178, 187-193.

10. Lek, M., Karczewski, K.J., Minikel, E.V., Samocha, K.E., Banks, E., Fennell, T., O'Donnell-Luria, A.H., Ware, J.S., Hill, A.J., Cummings, B.B., et al. (2016). Analysis of protein-coding genetic variation in 60,706 humans. Nature 536, 285-291.

11. Kircher, M., Witten, D.M., Jain, P., O'Roak, B.J., Cooper, G.M., and Shendure, J. (2014). A general framework for estimating the relative pathogenicity of human genetic variants. Nat Genet 46, 310-315.

12. Kremer, L.S., Bader, D.M., Mertes, C., Kopajtich, R., Pichler, G., Iuso, A., Haack, T.B., Graf, E., Schwarzmayr, T., Terrile, C., et al. (2017). Genetic diagnosis of Mendelian disorders via RNA sequencing. Nat Commun 8, 15824.

13. Griffin, H.R., Pyle, A., Blakely, E.L., Alston, C.L., Duff, J., Hudson, G., Horvath, R., Wilson, I.J., Santibanez-Koref, M., Taylor, R.W., et al. (2014). Accurate mitochondrial DNA sequencing using off-target reads provides a single test to identify pathogenic point mutations. Genet Med 16, 962-971.

14. Plagnol, V., Curtis, J., Epstein, M., Mok, K.Y., Stebbings, E., Grigoriadou, S., Wood, N.W., Hambleton, S., Burns, S.O., Thrasher, A.J., et al. (2012). A robust model for read count data in exome sequencing experiments and implications for copy number variant calling. Bioinformatics 28, 2747-2754.